ACS MEASUREMENT SCIENCE Au
AN OPEN ACCESS JOURNAL OF THE AMERICAN CHEMICAL SOCIETY

pubs.acs.org/measureau
Article

Sensing Liquid- and Gas-Phase Hydrocarbons via Mid-Infrared Broadband Femtosecond Laser Source Spectroscopy

Michael Hlavatsch,[#] Andrea Teuber,[#] Max Eisele, and Boris Mizaikoff[*]

Cite This: *ACS Meas. Sci. Au* 2023, 3, 452−458
Read Online
ACCESS | Metrics & More | Article Recommendations

ABSTRACT: In this study, we demonstrate the combination of a tunable broadband mid-infrared (MIR) femtosecond laser source separately coupled to a ZnSe crystal horizontal attenuated total reflection (ATR) sensor cell for liquid phase samples and to a substrate-integrated hollow waveguide (iHWG) for gas phase samples. Utilizing this emerging light source technology as an alternative MIR radiation source for Fourier transform infrared (FTIR) spectroscopy opens interesting opportunities for analytical applications. In a first approach, we demonstrate the quantitative analysis of three individual samples, ethanol (liquid), methane (gas), and 2-methyl-1-propene (gas), with limits of detection of 0.3% (ethanol) and 22 ppm_v and 74 ppm_v (methane and isobutylene), respectively, determined at selected emission wavelengths of the MIR laser source (i.e., 890 cm^{-1}, 1046 and 1305 cm^{-1}). Hence, the applicability of a broadband MIR femtosecond laser source as a bright alternative light source for quantitative analysis via FTIR spectroscopy in various sensing configurations has been demonstrated.

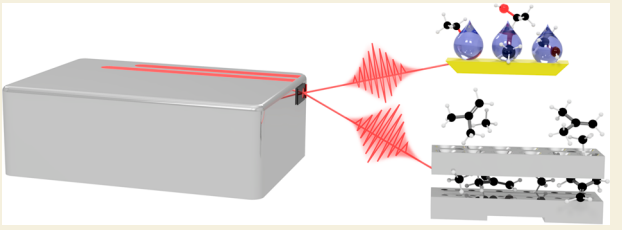

KEYWORDS: *Infrared laser spectroscopy, Attenuated total reflection, Substrate-integrated hollow waveguide, Er:fiber based laser, Tunable broadband mid-infrared femtosecond laser*

INTRODUCTION

Most of the fundamental vibrational, rovibrational, and rotational transitions of solids, liquids, and gases are found in the mid-infrared (MIR) range from 400 to 4000 cm^{-1} (2.5−25 μm; 12−120 THz).[1] These absorption patterns are molecule-specific, the so-called 'molecular fingerprints', and are therefore used for the identification and quantification of molecular analytes.[2] This makes MIR spectroscopy one of the most widely used and applied methods for the characterization and analysis of chemical components in fields such as material science,[3] medicine,[4−6] biotechnology,[7,8] and environmental analysis.[9−11] Therefore, the development of light sources in the MIR range has been continuously advanced in recent years. In particular, recent advances and the availability of novel laser sources in the mid-infrared range, such as quantum cascade lasers (QCL) and interband cascade lasers (ICL) lead overall to progress in the field of infrared spectroscopy.[12−14] While these lasers can be used to select individual, analyte-specific vibrational absorption lines, they are limited to a relatively small tuning range.

However, for a number of analytical applications, a compromise between broadband and narrowband IR absorption spectroscopy is required to adequately investigate complex samples with a limited number of compounds. This requirement can be met by using high-frequency comb laser sources. These are coherent light sources that emit a broad optical spectrum of equidistant frequencies. Using these equidistant frequencies within the frequency comb, narrowband absorption bands of molecules can be excited to obtain fine spectrally resolved information. Recent research with such light sources has already shown that frequency comb technology is an emerging field for applications in the MIR spectral region.[15−17] Especially, the use of fiber lasers doped with rare earth materials (e.g., ytterbium (Yb), erbium (Er), dysprosium (Dy)) for optical parametric oscillation and difference-frequency generation (DFG) are commonly used in frequency comb systems for the MIR light generation.[18−21] Keilmann and Amarie[19] developed an interesting laser frequency comb system based on a 100 fs Er-doped fiber laser pulse train with 1.55 μm wavelength, which is then mixed with supercontinuum pulses with wavelengths between 1.7 and 2.3 μm. During mixing, both output beams are focused on a GaSe crystal in the DFG unit and mixed to produce a mid-infrared continuous beam. By subsequent coupling of the MIR beam into a Michelson interferometer, spectrally resolved information can be generated over a wide spectral window. The tunability and relatively wide spectral range of this

Received: June 21, 2023
Revised: September 4, 2023
Accepted: September 5, 2023
Published: October 12, 2023

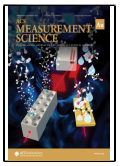

frequency comb laser source coupled with DFG render it suitable for analytical applications using Fourier transform infrared spectroscopy (FTIR).

For FTIR spectroscopy and a variety of other spectroscopic applications, an optical waveguide can be used to ensure intimate interaction of photons with the sample constituents. For example, in attenuated total reflection (ATR) spectroscopy, light propagates in an internal reflecting element (IRE), e.g., a zinc selenide (ZnSe) crystal, whereby at each sample−crystal junction, an evanescent field penetrating into the sample medium is emerging. At these hotspots, light penetrates the sample medium with a penetration depth of several micrometers and gets absorbed.[2,22,23] For gaseous samples, on the other hand, a combination of a waveguide and an efficient miniaturized gas cell is needed. Such a combination was first applied in the 1980s by Griffith et al.[24] called a hollow waveguide (HWG). An elegant solution for combining highly miniaturized gas cells with efficient photonic waveguides has recently been developed by Mizaikoff and colleagues: the so-called substrate-integrated hollow waveguides (iHWGs). iHWGs combine both gas cell and waveguide enabling to address transient signals from small gas volumes with excellent signal-to-noise ratio in gas absorption measurements.[25−27]

In this study, we report the combination of an Er:fiber-based femtosecond mid-infrared laser source serving as a light source in FTIR spectroscopy of liquid and gaseous samples using a ZnSe IRE waveguide for in situ liquid-phase infrared measurements in a horizontal attenuated total internal reflection (hATR) configuration and an iHWG for laser absorption spectroscopy (LAS) in the gas phase, respectively. The respective combinations have been used for the detection of liquid and gaseous hydrocarbons at low concentrations, paving the way for quantitative spectroscopic analysis of fast chemical reactions in the mid-infrared regime.

MATERIALS AND METHODS

Experimental Setup

The optical setup is schematically shown in Figure 1, where two separate pathways are shown. The first beam path (red line) is the broadband MIR femtosecond laser source (TOPTICA Photonics AG, Gräfelfing, Germany), and the second one (dashed yellow line) is the beam path of the blackbody radiator (globar) of the FTIR Vertex70 (Bruker Optik GmbH, Ettlingen, Germany). When using the femtosecond laser source, the beam was directed into the Vertex70 via a planar gold mirror through the Michelson interferometer into the sample chamber. There, it was coupled into the respective coupling facets of the different sensing assemblies, i.e., hATR (liquid samples) or iHWG (gaseous samples). In the case of liquid samples, the radiation was focused on the facet of a horizontal ATR (hATR, Bruker Optics, Ettlingen, Germany) transducer equipped with a ZnSe IRE (72 × 10 × 6 mm^3 (L × W × H) with a 45° in- and out-coupling facet angle). For gas measurements, the radiation was focused into a 75 mm straight-channel iHWG. After the laser light source radiation propagated through respective waveguides, the radiation emerging at the distal end (orange line in Figure 1) was focused directly onto a liquid-nitrogen-cooled mercury cadmium telluride (MCT) detector (InfraRed Associates Inc., Stuart, FL, USA) with an active detector element area of 4 mm^2.

To compare the laser source with the blackbody radiator of the FTIR spectrometer, the laser source light was switched off, and IR radiation emitted by the globar was directed through the interferometer onto the sample using an 8 mm aperture. The remaining optics and respective waveguides were handled as described previously.

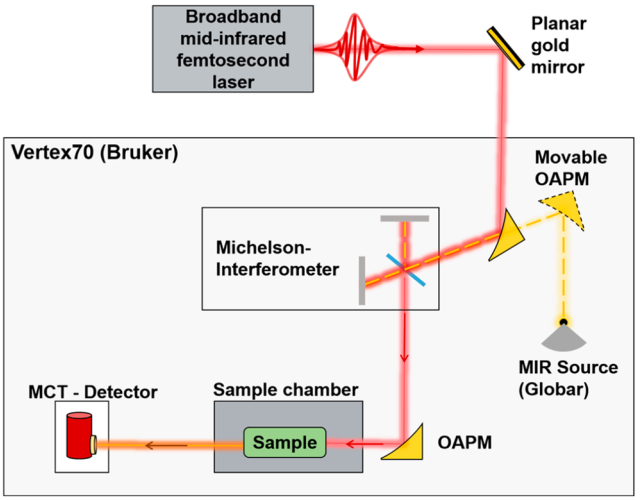

Figure 1. Schematic illustration of the experimental setup for the broadband mid-infrared femtosecond laser system (red line: laser source beam; yellow dashed line: globar radiation; OAPM: off-axis parabolic mirror; orange line: attenuated light after sample interaction MCT detector: mercury cadmium telluride detector).

Measurement Procedure

Liquid Sample Preparation. In the first approach, ethanol (C_2H_6O, ≥ 99.5%; VWR International GmbH, Darmstadt, Germany) and Milli-Q water were measured. In the second step, a stock solution with an initial concentration of 40% was prepared, and from this, concentrations in the range of 0.08 to 10% were prepared via a dilution series.

After recording the background, 1.5 μL of each analyte solution was measured five times with the hATR cell starting from the lowest to highest concentration. Each concentration was measured five times. Between each sample change, the same appropriate cleaning steps (rinsing with water, drying, and rinsing with the new solution) were conducted.

Gas Sample Preparation. For the gas-phase experiments, certified gas standards of isobutylene (2-methyl-1-propene, *i*-C_4H_8; 1.0% isobutylene in N_2, Westfalen AG, Münster, Germany) and methane (CH_4; 1.0% methane in N_2, Westfalen AG, Münster, Germany) were diluted with nitrogen (99.9% N_2, MTI IndustrieGase AG, Neu-Ulm, Germany) to mixtures in the concentration range between 100 to 1000 ppm_v in a customized gas mixing system (GMS) based on mass flow controllers developed in collaboration with Lawrence Livermore National Laboratory (LLNL; Livermore/CA, USA) and directly fed into the iHWG.

Prior to each measurement, the iHWG was purged using nitrogen gas for 5 min at a flow rate of 200 mL/min. After recording the background spectra, the defined gas mixture was set at the gas mixing system, and the flow-through cell was flushed with the specified sample concentration at a flow rate of 200 mL/min for 3 min. Subsequently, five repeated sample measurements were conducted. After the IR spectra of the sampled concentration were recorded, the gas flow was purged with nitrogen.

Data Acquisition and Evaluation. The software package OPUS 8.1 (Bruker Optik GmbH, Ettlingen, Germany) was used for the IR data acquisition and processing. Each IR spectrum was recorded in a custom spectral range matched to the analyte used with a resolution of 2 cm^{-1} using a Blackman−Harris three-term apodization function and an average of 128 scans. The measured analytes and respective spectral ranges are shown in Table 1.

The performance of the broadband MIR femtosecond laser source regarding its applicability was quantified by calculating calibration functions in the concentration range of 0.04 to 10% for liquid samples and in the concentration range of 100 to 1000 ppm_v for gas samples. The limit of detection (LOD) and limit of quantification (LOQ) of

https://doi.org/10.1021/acsmeasuresciau.3c00026
ACS Meas. Sci. Au 2023, 3, 452−458

Table 1. Recorded Spectral Range of the Laser Source, Analyzed Peak Positions, Integrated Peak Area, and Set Baseline Correction Points for the Respective Analyzed Liquid Sample (Ethanol) and Gas Samples (Methane and Isobutylene)

Analyte	Spectr. range [cm^{-1}]	Peak [cm^{-1}]	Integrated peak area [cm^{-1}]	Baseline correction
Ethanol	1200−950	1046[28]	1065−1015	1065, 1015
Methane	1450−1150	1305[29]	1308−1301	1308, 1301
Isobutylene	1050−750	890[30]	894−882	894, 882

the respective samples were determined by calculating the integrated areas of the peaks given in Table 1. Prior applied baseline corrections and area calculations were performed by using the Essential eFTIR spectroscopy software toolbox (Essential FTIR, Madison WI, USA). Subsequently, the linear correlation, the confidence interval, and the prediction interval were calculated according to the approach of Hubaux and Vos.[31]

Equipment

Horizontal Attenuated Total Reflection Assembly. To measure liquid samples in FTIR spectroscopy, the hATR cell equipped with a ZnSe crystal plate (Spectral Systems LLC, Hopewell Junction/NY, USA), with dimensions of 72 × 10 × 6 mm^3 (L × W × H), with an input and output coupling angle of 45° was used. The hATR cell was equipped with a self-assembled sample plate with sample volumes up to 2 mL. To guide the light into the ZnSe crystal, four plane mirrors are used, two before and two after the crystal; see Figure 2a.

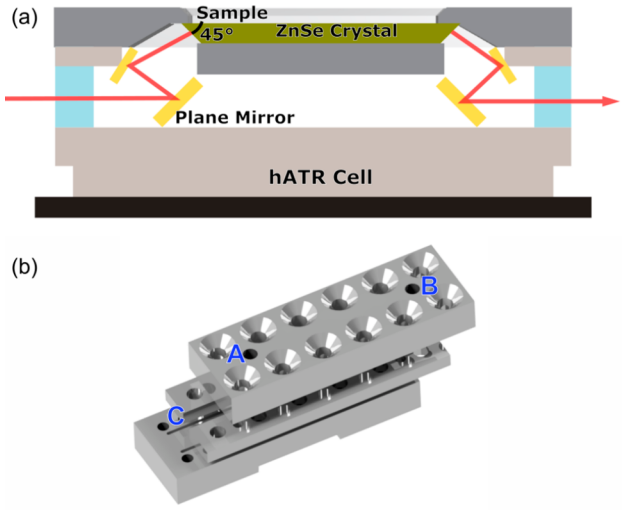

Figure 2. (a) Schematic cross section of the infrared horizontal attenuated total reflection (hATR) measurement cell with four mirrors guiding the incident laser source light through the ZnSe crystal plate on top of the cell. (b) Cross-section of an open iHWG with (A) gas inlet, (B) gas outlet, and (C) wave guiding channel.

Substrate-Integrated Hollow Waveguide. The iHWG (75 × 25 × 20 mm^3, L × W × H) used in this study (Figure 2b) was produced from an aluminum substrate. It provides an optical path length of 70 mm with a squared cross-section of 4 × 4 mm^2. The cover substrate (top) has two threaded ports that serve as gas inlets and outlets to the iHWG channel (Figure 2b, A and B). Both the substrate top and bottom surfaces were polished to a mirror-like surface with commercially available diamond polishing suspensions, ensuring a high surface reflectivity. All four parts were glued with epoxy and screwed together to ensure a gas-tight connection. Both ends were sealed gas-tight with MIR-transparent BaF_2 windows, resulting in a minute sample volume of 1120 μL.

RESULTS AND DISCUSSION

First, the characteristic spectral range of the laser source can be seen in Figure 3, with its wavelength range from 20 THz to 60

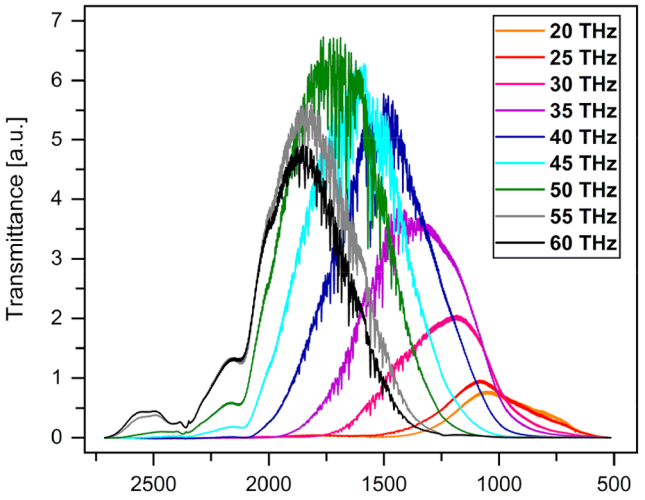

Figure 3. Characteristic emission of the broadband mid-infrared femtosecond laser in the range from 20 to 60 THz (2000−667 cm^{-1}) with 5 THz increments recorded with the FTIR spectrometer.

THz (2000−667 cm^{-1}) with 5 THz incrementing steps. As shown in this figure, the laser light source has its highest intensity at ∼50 THz (1667 cm^{-1}) and decreases toward the edges, being much stronger toward 20 THz (667 cm^{-1}).

Comparison of Laser Source vs Globar

Figure 4 shows the absorption spectra of water (Figure 4a) and ethanol (Figure 4b) with their respective vibrational and rovibrational transitions covering different spectral regions of the broadband MIR laser source. For the water sample (Figure 4a), the wavenumber at the laser source was set to 1667 cm^{-1} (H−O−H bending),[32] and for ethanol (Figure 4b), it was set to 1046 cm^{-1} (C−O stretch). Zooming into the region around the selected wavenumber for the respective sample (inset plots), it is evident that the intensity of the laser source for the selected wavenumber in the region of interest is higher in comparison to the globar radiation source. The high noise level for wavenumbers > 2000 cm^{-1} is due to this region being outside the spectral tuning range of the laser source (see Figure 3). This initial comparison indicates the suitability and applicability of the laser source for quantitative analytical studies.

Liquid Sample Analysis

For quantitative analysis using the broadband MIR femtosecond laser source of a liquid sample, ethanol was analyzed and evaluated based on its C−O peak at 1046 cm^{-1} (see Table 1).

In Figure 5a and b, the calibration functions for two separately executed ethanol measurements in the concentration range of 0.08 to 10% with their respective LOD and LOQ values are displayed. For both measurements, the integrated peak area shows a linear response to the increase in concentration, which is in very good agreement with Beer−Lambert's law. Furthermore, the linear regressions of both independent measurements show a coefficient of determination (R^2) of > 0.99, confirming the suitability of the calibration model for quantitative analysis.

https://doi.org/10.1021/acsmeasuresciau.3c00026
ACS Meas. Sci. Au 2023, 3, 452−458

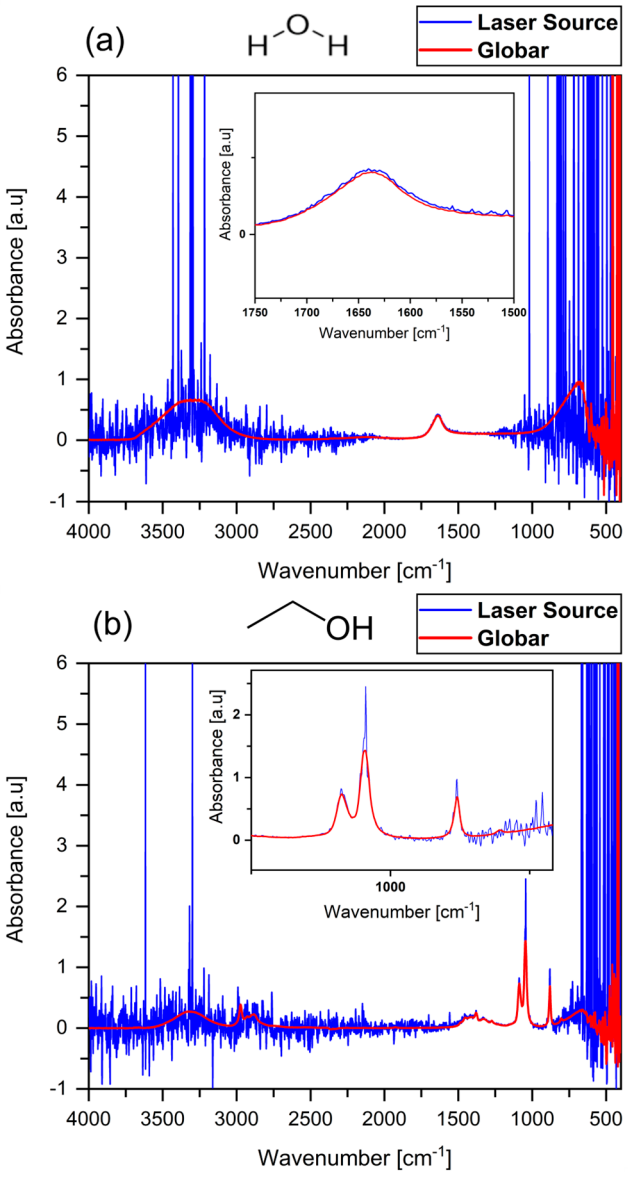

Figure 4. Comparison between the broadband mid-infrared femtosecond laser source and the globar radiation source of the Vertex70 with the laser source focusing on the respective selected peak wavenumbers: (a) water: $\bar{\nu}$ = 1667 cm^{-1} and (b) ethanol: $\bar{\nu}$ = 1046 cm^{-1}.

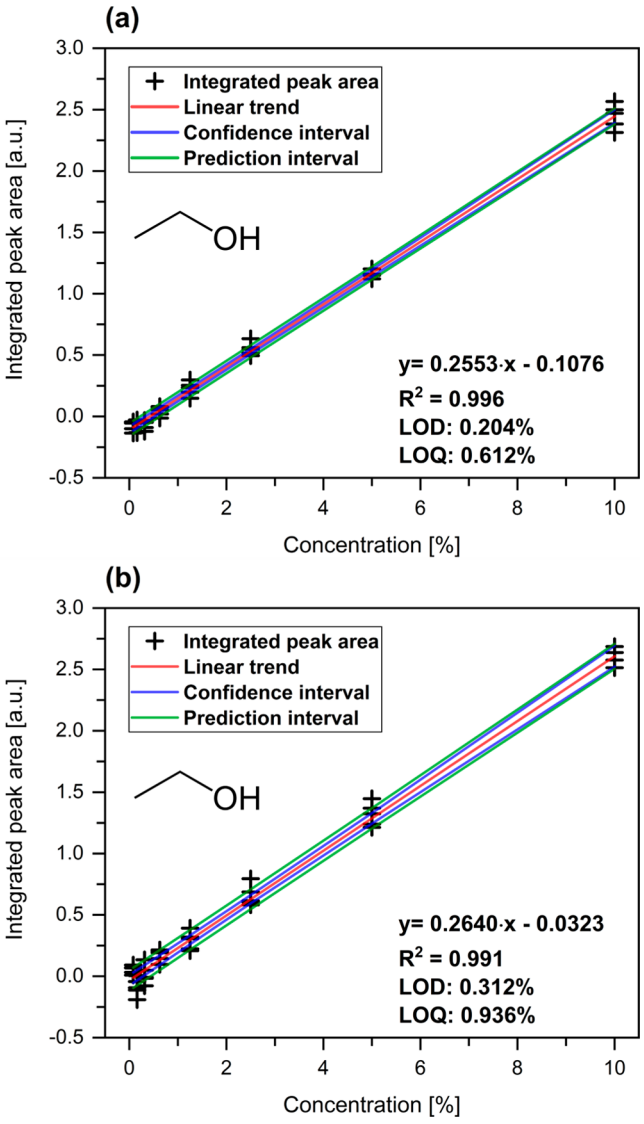

Figure 5. Linear correlation between the integrated peak area and the concentration ranging from 0.08 to 10% of two independent ethanol measurements (a and b) with their calculated linear regression equation, coefficient of determination (R2), and LOD and LOQ values.

Despite a relatively large difference in LOQ between the two measurements, which can be explained due to temperature fluctuations, the broadband MIR femtosecond laser source can accurately determine ethanol concentrations in the subpercent range and even detect them in the per mil range based on the LOD values. These LOD and LOQ values are seven times lower compared to the LOD and LOQ values of the measurements with the global radiation source. This discrepancy can be explained by the fact that the spectrometer as a whole system is optimized for each of its optical parts. This may not be the case with the external coupling of the laser light source into the interferometer and, therefore, is less optimized.

Gas Sample Analysis

The femtosecond MIR laser source can be used not only for liquid analytes but also for a wide range of gaseous analytes, such as methane and isobutylene, with gas concentrations in the range of 100−1000 ppm_v.

Methane Studies

For the analysis of the rovibrational transitions of methane, the laser source was set to 1305 cm^{-1}, and calibration functions were calculated according to the spectral ranges; see Table 1.

As evident in Figure 6a and b, the integrated peak area increases linearly with the measured methane concentration (100−1000 ppm_v) following Beer−Lambert's law. Furthermore, the calibration functions for the two individual methane measurements exhibit accuracy, with R^2 values exceeding 0.99. This noteworthy degree of correlation highlights the linear calibration model and confirms its suitability for precise quantitative analysis using the femtosecond laser source. Furthermore, these results provide first evidence that the broadband MIR femtosecond laser source enables spectroscopic analysis of both liquid and gaseous samples, demonstrating its versatility and broad applicability. In

https://doi.org/10.1021/acsmeasuresciau.3c00026
ACS Meas. Sci. Au 2023, 3, 452−458

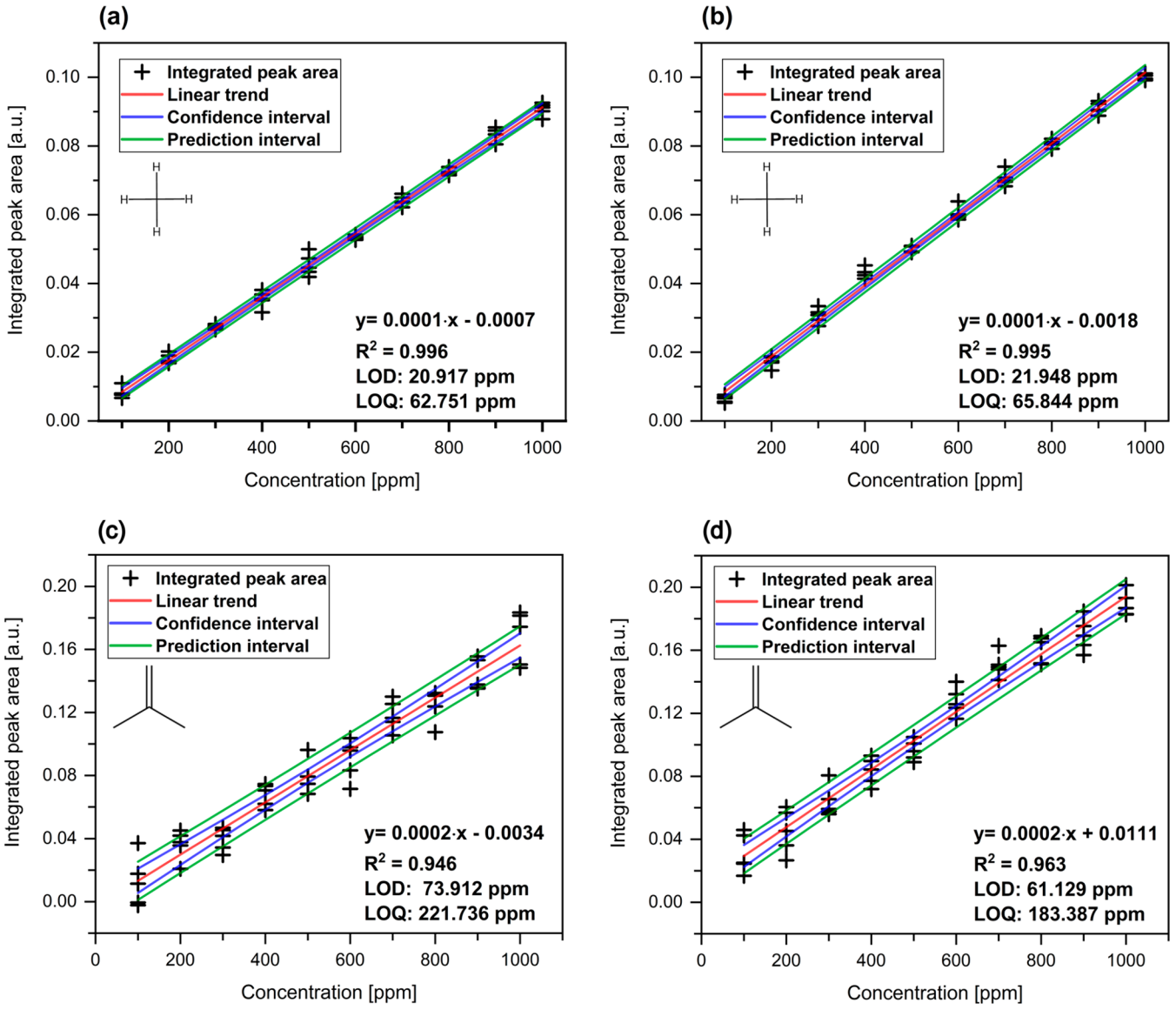

Figure 6. Linear correlation between the integrated peak area and the concentration ranging from 100 to 1000 ppm_v of two independent measurements with respective LOD, LOQ, and R^2 values for (a, b) methane and (c, d) isobutylene.

addition, considering measurement errors, the independent measurements show concordant LOD and LOQ values, allowing quantitative analysis of methane in the 60 to 70 ppm_v range.

Isobutylene Studies

Besides methane, isobutylene was analyzed as a second exemplary analyte. The C═CH_2 vibration of isobutylene at 890 cm^{-1} was measured at a different central wavenumber and with a lower output power compared to the previous measurement. For power quantification, the LOD and LOQ values for the peaks and spectral regions were calculated according to Table 1.

Figure 6c and d display the integrated peak area plotted against the concentration in the range of 100−1000 ppm_v, which again is described by a linear correlation. In contrast to the calibration functions shown previously, the calibration functions of the two individual isobutylene measurements have lower R^2 values of between 0.94 and 0.97. This aberrancy, as well as the variations in LOD and LOQ values between the measurements, can be explained by the weaker laser light source intensity (see Figure 3) at 890 cm^{-1}, at which less interaction between light and the sample occurs. Despite the lower power at 890 cm^{-1}, isobutylene can be detected at a concentration of about 70 ppm_v and determined at a concentration of approximately 240 ppm_v with the broadband MIR femtosecond laser source. It can be concluded that the evaluated data are sufficiently well described by the linear model and are suitable for quantitative spectroscopic analysis. Furthermore, when comparing the LOD and LOQ values for the respective gas measurements, the LODs and LOQs for methane are approximately 10.5 times lower and those for isobutylene approximately 12 times lower compared to the LOD and LOQ values of the measurements with the global radiation source, respectively. Again, this discrepancy can be explained by the fact that the spectrometer is optimized as a whole system, which may not be the case for external coupling. In addition, the light is not coupled into the iHWG at a specific angle, unlike the hATR liquid sample cell, resulting in fewer

https://doi.org/10.1021/acsmeasuresciau.3c00026
ACS Meas. Sci. Au 2023, 3, 452−458

possible bounces and subsequently fewer light−sample interactions.

CONCLUSIONS

In this study, we demonstrated the combination of a broadband femtosecond mid-infrared laser source with a ZnSe IRE sensor cell for in situ IR-ATR spectroscopy of liquid phase samples and with an iHWG for gas-phase sensing applications. Three exemplary analytes—ethanol (liquid), methane (gas) and isobutylene (gas)—were detected and quantified in a first application example of this laser light source in FTIR spectroscopy. We demonstrated that the broadband femtosecond laser source in the mid-infrared range provides an alternative MIR radiation source for the quantitative analysis of samples in both the liquid and gas phase using exceedingly small sample volumes in the low percentage concentration range for liquid samples and in the mid ppm_v range for gas samples, which were reliably detected and quantified.

As a possible future prospect, the femtosecond pulse characteristics of the laser source in the mid-infrared range may be utilized for studying ultrafast chemical reaction dynamics. Examples include but are not limited to reaction-oriented electrochemistry for the investigation of single- and multiple-electron-transfer processes and very fast redox reactions.

AUTHOR INFORMATION

Corresponding Author

Boris Mizaikoff − *Institute of Analytical and Bioanalytical Chemistry, Ulm University, D-89081 Ulm, Germany; Hahn-Schickard, D-89077 Ulm, Germany;* orcid.org/0000-0002-5583-7962; Phone: +49-731-50-22751; Email: boris.mizaikoff@uni-ulm.de; Fax: +49-731-50-22763

Authors

Michael Hlavatsch − *Institute of Analytical and Bioanalytical Chemistry, Ulm University, D-89081 Ulm, Germany*

Andrea Teuber − *Institute of Analytical and Bioanalytical Chemistry, Ulm University, D-89081 Ulm, Germany*

Max Eisele − *TOPTICA Photonics AG, D-82166 Graefelfing (Munich), Germany*

Complete contact information is available at: https://pubs.acs.org/10.1021/acsmeasuresciau.3c00026

Author Contributions

#M.H. and A.T. contributed equally. M.H. and A.T. conceived, designed and performed the experiments, analyzed the data, and wrote and reviewed the article. B.M. supervised the experiments. M.E. and B.M. reviewed and edited the article. All authors have read and agreed to the published version of the manuscript. CRediT: **Michael Hlavatsch** conceptualization, data curation, formal analysis, investigation, methodology, validation, visualization, writing-original draft; **Andrea Teuber** conceptualization, data curation, formal analysis, investigation, methodology, validation, visualization, writing-original draft; **Max Eisele** resources, writing-review & editing; **Boris Mizaikoff** funding acquisition, resources, writing-review & editing.

Funding

This study was supported in part by the DFG Graduiertenkolleg PULMOSENS (GRK 2203), and by the by the Ministerium für Wissenschaft, Forschung and Kunst (MWK) in Baden-Württemberg, Germany via the program "Sonderförderlinie COVID-19" within project IRENE.

Notes

The authors declare no competing financial interest.

ACKNOWLEDGMENTS

The authors want to acknowledge valuable support from their colleagues from the Institute of Analytical and Bioanalytical Chemistry (IABC) at Ulm University. The Machine Shop at Ulm University is thanked for support during prototyping and development.

ABBREVIATIONS

MIR, mid-infrared; iHWG, substrate-integrated hollow waveguide; FTIR, Fourier transform infrared spectroscopy; QCL, quantum cascade laser; ICL, interband cascade lasers; DFG, difference-frequency generation; ATR, attenuated total reflection; IRE, internal reflecting element; ZnSe, zinc selenide; IR-hATR, horizontal attenuated total internal reflection; LAS, laser absorption spectroscopy; LOD, limit of detection; LOQ, limit of quantification

REFERENCES

(1) Griffiths, P. R.; de Haseth, J. A. *Fourier Transform Infrared Spectrometry*; John Wiley & Sons, Inc: Hoboken, NJ, USA, 2007. .

(2) Mizaikoff, B. Waveguide-Enhanced Mid-Infrared Chem/Bio Sensors. *Chem. Soc. Rev.* **2013**, *42* (22), 8683.

(3) Willer, U.; Saraji, M.; Khorsandi, A.; Geiser, P.; Schade, W. Near- and Mid-Infrared Laser Monitoring of Industrial Processes, Environment and Security Applications. *Opt Lasers Eng.* **2006**, *44* (7), 699−710.

(4) Tütüncü, E.; Mizaikoff, B. Cascade Laser Sensing Concepts for Advanced Breath Diagnostics. *Anal Bioanal Chem.* **2019**, *411* (9), 1679−1686.

(5) Hou, S.; Riley, C. B.; Mitchell, C. A.; Shaw, R. A.; Bryanton, J.; Bigsby, K.; McClure, J. T. Exploration of Attenuated Total Reflectance Mid-Infrared Spectroscopy and Multivariate Calibration to Measure Immunoglobulin G in Human Sera. *Talanta* **2015**, *142*, 110−119.

(6) Pandey, R.; Dingari, N. C.; Spegazzini, N.; Dasari, R. R.; Horowitz, G. L.; Barman, I. Emerging Trends in Optical Sensing of Glycemic Markers for Diabetes Monitoring. *TrAC Trends in Analytical Chemistry* **2015**, *64* (1), 100−108.

(7) Kansiz, M.; Billman-Jacobe, H.; McNaughton, D. Quantitative Determination of the Biodegradable Polymer Poly(β-Hydroxybutyrate) in a Recombinant Escherichia Coli Strain by Use of Mid-Infrared Spectroscopy and Multivariative Statistics. *Appl. Environ. Microbiol.* **2000**, *66* (8), 3415−3420.

(8) Estevez, M. C.; Alvarez, M.; Lechuga, L. M. Integrated Optical Devices for Lab-on-a-Chip Biosensing Applications. *Laser Photon Rev.* **2012**, *6* (4), 463−487.

(9) Reidl-Leuthner, C.; Ofner, J.; Tomischko, W.; Lohninger, H.; Lendl, B. Simultaneous Open-Path Determination of Road Side Mono-Nitrogen Oxides Employing Mid-IR Laser Spectroscopy. *Atmos. Environ.* **2015**, *112* (2), 189−195.

(10) Nikodem, M.; Wysocki, G. Chirped Laser Dispersion Spectroscopy for Remote Open-Path Trace-Gas Sensing. *Sensors* **2012**, *12* (12), 16466−16481.

(11) Jouy, P.; Mangold, M.; Tuzson, B.; Emmenegger, L.; Chang, Y.-C.; Hvozdara, L.; Herzig, H. P.; Wägli, P.; Homsy, A.; de Rooij, N. F.; Wirthmueller, A.; Hofstetter, D.; Looser, H.; Faist, J. Mid-Infrared

Spectroscopy for Gases and Liquids Based on Quantum Cascade Technologies. *Analyst* **2014**, *139* (9), 2039−2046.
(12) Spagnolo, V.; Kosterev, A. A.; Dong, L.; Lewicki, R.; Tittel, F. K. NO Trace Gas Sensor Based on Quartz-Enhanced Photoacoustic Spectroscopy and External Cavity Quantum Cascade Laser. *Appl. Phys. B: Laser Opt.* **2010**, *100* (1), 125−130.
(13) Sieger, M.; Haas, J.; Jetter, M.; Michler, P.; Godejohann, M.; Mizaikoff, B. Mid-Infrared Spectroscopy Platform Based on GaAs/AlGaAs Thin-Film Waveguides and Quantum Cascade Lasers. *Anal. Chem.* **2016**, *88* (5), 2558−2562.
(14) Lehtinen, J.; Kuusela, T. Broadly Tunable Quantum Cascade Laser in Cantilever-Enhanced Photoacoustic Infrared Spectroscopy of Solids. *Appl. Phys. B: Laser Opt.* **2014**, *115* (3), 413−418.
(15) Schliesser, A.; Picqué, N.; Hänsch, T. W. Mid-Infrared Frequency Combs. *Nat. Photonics* **2012**, *6* (7), 440−449.
(16) Udem, Th.; Holzwarth, R.; Hänsch, T. W. Optical Frequency Metrology. *Nature* **2002**, *416* (6877), 233−237.
(17) Burghoff, D.; Kao, T.-Y.; Han, N.; Chan, C. W. I.; Cai, X.; Yang, Y.; Hayton, D. J.; Gao, J.-R.; Reno, J. L.; Hu, Q. Terahertz Laser Frequency Combs. *Nat. Photonics* **2014**, *8* (6), 462−467.
(18) Krauss, G.; Lohss, S.; Hanke, T.; Sell, A.; Eggert, S.; Huber, R.; Leitenstorfer, A. Synthesis of a Single Cycle of Light with Compact Erbium-Doped Fibre Technology. *Nat. Photonics* **2010**, *4* (1), 33−36.
(19) Keilmann, F.; Amarie, S. Mid-Infrared Frequency Comb Spanning an Octave Based on an Er Fiber Laser and Difference-Frequency Generation. *J. Infrared Millim Terahertz Waves* **2012**, *33* (5), 479−484.
(20) Ruehl, A.; Gambetta, A.; Hartl, I.; Fermann, M. E.; Eikema, K. S. E.; Marangoni, M. Widely-Tunable Mid-Infrared Frequency Comb Source Based on Difference Frequency Generation. *Opt. Lett.* **2012**, *37* (12), 2232.
(21) Leindecker, N.; Marandi, A.; Byer, R. L.; Vodopyanov, K. L.; Jiang, J.; Hartl, I.; Fermann, M.; Schunemann, P. G. Octave-Spanning Ultrafast OPO with 26−61μm Instantaneous Bandwidth Pumped by Femtosecond Tm-Fiber Laser. *Opt Express* **2012**, *20* (7), 7046.
(22) Harrick, N. J. SURFACE CHEMISTRY FROM SPECTRAL ANALYSIS OF TOTALLY INTERNALLY REFLECTED RADIATION *. *J. Phys. Chem.* **1960**, *64* (9), 1110−1114.
(23) Blum, M.-M.; John, H. Historical Perspective and Modern Applications of Attenuated Total Reflectance - Fourier Transform Infrared Spectroscopy (ATR-FTIR). *Drug Test Anal* **2012**, *4* (3−4), 298−302.
(24) Griffiths, P. R.; Pentoney, S. L.; Giorgetti, A.; Shafer, K. H. The HYPHENATION of CHROMATOGRAPHY & FT-IR SPECTROMETRY. *Anal. Chem.* **1986**, *58* (13), 1349A−1366A.
(25) Wilk, A.; Carter, J. C.; Chrisp, M.; Manuel, A. M.; Mirkarimi, P.; Alameda, J. B.; Mizaikoff, B. Substrate-Integrated Hollow Waveguides: A New Level of Integration in Mid-Infrared Gas Sensing. *Anal. Chem.* **2013**, *85* (23), 11205−11210.
(26) Barreto, D. N.; Silva, W. R.; Mizaikoff, B.; da Silveira Petruci, J. F. Monitoring Ozone Using Portable Substrate-Integrated Hollow Waveguide-Based Absorbance Sensors in the Ultraviolet Range. *ACS Measurement Science Au* **2022**, *2* (1), 39−45.
(27) Perez-Guaita, D.; Kokoric, V.; Wilk, A.; Garrigues, S.; Mizaikoff, B. Towards the Determination of Isoprene in Human Breath Using Substrate-Integrated Hollow Waveguide Mid-Infrared Sensors. *J. Breath Res.* **2014**, *8* (2), No. 026003.
(28) Corsetti, S.; McGloin, D.; Kiefer, J. Comparison of Raman and IR Spectroscopy for Quantitative Analysis of Gasoline/Ethanol Blends. *Fuel* **2016**, *166*, 488−494.
(29) Ogilvie, J. F.; Chou, S.-L.; Lin, M.-Y.; Cheng, B.-M. Mid-Infrared Spectra of Methane Dispersed in Solid Neon and Argon. *Vib Spectrosc* **2011**, *57* (2), 196−206.
(30) Radziszewski, J. G.; Arrington, C. A.; Downing, J. W.; Balaji, V.; Murthy, G. S.; Michl, J. Vibrational Transition Moment Directions in Medium-Size Molecules: Experiment and Theory. *Journal of Molecular Structure: THEOCHEM* **1988**, *163*, 191−206.
(31) Hubaux, A.; Vos, G. Decision and Detection Limits for Calibration Curves. *Anal. Chem.* **1970**, *42* (8), 849−855.
(32) Morita, M.; Matsumura, F.; Shikata, T.; Ogawa, Y.; Kondo, N.; Shiraga, K. Hydrogen-Bond Configurations of Hydration Water around Glycerol Investigated by HOH Bending and OH Stretching Analysis. *J. Phys. Chem. B* **2022**, *126* (47), 9871−9880.

https://doi.org/10.1021/acsmeasuresciau.3c00026
ACS Meas. Sci. Au 2023, 3, 452−458